Engineering Structures 179 (2019) 204–210

Contents lists available at ScienceDirect

Engineering Structures

journal homepage: www.elsevier.com/locate/engstruct

# An experimental evaluation of the blast resistance of heterogeneous concrete-based composite bridge decks

Radek Hajek[a], Josef Fladr[a], Jiri Pachman[b], Jiri Stoller[c], Marek Foglar[a,*]

[a] Czech Technical University in Prague, Faculty of Civil Engineering, Department of Concrete and Masonry Structures, Prague, Czech Republic
[b] University of Pardubice, Faculty of Chemical Technology, Institute of Energetic Materials, Pardubice, Czech Republic
[c] University of Defence, Faculty of Military Technology, Brno, Czech Republic

ARTICLE INFO

*Keywords:*
Blast performance
Heterogeneity
Layered composite

ABSTRACT

Because of the current geopolitical situation, research on improving the resistance of the civil and transport infrastructure to blast or impact loads has gained considerable attention. This paper presents the results of full-scale blast experiments designed to characterize the resistance of concrete-based composite bridge decks subjected to close-in blast loading. Three composite decks with different degrees of heterogeneity were proposed and tested: a slab with basalt fiber meshes in multiple layers along the depth of the specimen, a slab with recycled textile sheets 100 mm in total thickness, and a typical hollow-core prestressed slab. The dependence of the extent of the blast damage on the material characteristics of the composite material was studied. A detailed study of the damage to the specimen caused by the close-in explosion found apparent delamination of all tested composite specimens. The heterogeneity of the layered composite material converts the blast damage due to internal rebounds into layer delamination.

## 1. Introduction

Due to the current geopolitical situation, there has been a considerable increase in the number of terrorist acts in recent years. The need to improve the resistance to blast or to impact of the civil and transport infrastructure has led to increased interest in research and development on various materials, and on their resistance to high strain-rate loading.

This paper presents the results of a full-scale experimental program focused on the blast resistance of hybrid concrete specimens subjected to close-in blast loading, and the dependence of the resistance on the composition and the material properties of the specimen. This research program built on previous research conducted by the authors. Since 2010, the authors have been conducting experiments with an unchanged arrangement, using various types and compositions of concrete, ranging from normal-strength concrete without distributed reinforcement (NSC) to ultrahigh-performance fiber-reinforced concrete (UHPFRC). The results of earlier experiments are presented in [1–3]. To explore ways of further enhancing the blast resistance of concrete, the experiments presented in this paper introduced three specimens with an atypical internal structure made of newly-developed concrete-based composite materials utilizing basalt fiber meshes and recycled textile sheets. One conventional specimen with a hollow core was also used for comparison.

### 1.1. State-of-the-art on blast performance of composites

Shock wave propagation through a heterogeneous environment is a very complex issue, because the shock wave is partially reflected from and partially passes through any interface of environments with different densities. This partial reflection can effectively mitigate the effects of a blast wave.

This paper builds on the research on air shock wave propagation and interactions in heterogeneous environments previously conducted by the authors, see [4,5]. The use of heterogeneous materials in blast-resistant devices and structures can significantly increase their effectiveness. Composite building materials are generally well suited to achieve the required material heterogeneity.

The use of sandwich-structured composites for shielding against blast and impact is a usual approach. A combination of steel or other high-strength materials with softer materials, such as wood or plastic, has been widely used for a long time in the design of blast-resistant structures. The plastic deformation of a soft core can dissipate the energy of the blast wave and reduce the effect of an explosion. The mechanical properties of the soft core can have a significant impact on the behavior of the structure. Composites with three different polymeric

* Corresponding author at: ČVUT v Praze, Thákurova 7, 166 29 Praha 6, Czech Republic.
*E-mail address:* marek.foglar@fsv.cvut.cz (M. Foglar).

https://doi.org/10.1016/j.engstruct.2018.10.070
Received 3 April 2018; Received in revised form 6 October 2018; Accepted 24 October 2018
0141-0296/ 

foam cores for resistance to a 100 kg TNT equivalent charge at a standoff distance of 15 m were tested in [6]. The behavior of similar foam core glass-fiber-reinforced polymer (GFRP) composites subject to multiple explosive blasts was studied in [7].

Additional approaches and materials can be used to provide ductile behavior for otherwise brittle fiber-reinforced composites, for example a three-dimensional woven textile fabric [8].

### 1.2. State-of-the-art on blast performance of concrete-based composites

Despite recent innovations in the design of polymer-based composites, composites utilizing steel and concrete are the usual choice for use in the most robust applications. Concrete is a very widely used building material, due to its high durability, resistance to aggressive environments and relatively low financial cost. It usually has sufficient compressive strength to replace costlier construction steel, but its tensile strength is low in comparison with steel with essentially the same compressive and tensile strength. In past decades, many attempts have been made to improve the characteristics of concrete, so that it can be used to replace steel in many other applications. The improvements are usually made by introducing another material into the concrete matrix, which normally consists of aggregate, water and cement. These materials are chemically reacted to form a hard matrix. The first approach, which is still the most widely followed, uses steel reinforcing bars to provide tensile strength to the structure. However, this approach does not improve the tensile strength of the material. The tensile stresses are transferred to the reinforcement. The concrete surrounding the material usually fails in tension and cracks. The reinforcement holds the cracked concrete parts together.

Dispersed reinforcement in the form of fibers of various shapes and materials have been introduced to improve the tensile properties of the concrete matrix, and also to increase its fracture energy. Dispersed reinforcement is now in common use in structures to reduce the risk of the concrete cracking, and mainly to ensure the required durability of the structure.

The blast resistance of FRC with carbon fibers 100 mm in length was studied in [9]. The specimens were concrete slabs with dimensions of 1.83 × 1.83 × 0.165 m. A charge weight of 34 kg TNT (Trinitrotoluene) equivalent at a stand-off distance was used in a series of experiments. A significant increase in spall and breach resistance was found for the FRC specimens. The blast resistance of steel fiber reinforced concrete (SFRC) has also been studied by other authors [10–13].

Together with increased compressive strength, UHPFRC generally also has greater tensile strength than a usual concrete. The increase in tensile strength can be ascribed to the presence of the dispersed steel reinforcement. Measurements are typically made of the flexural tensile strength of concrete, instead of measurements of the direct tensile strength. Direct tension tests of concrete, especially FRC, are hard to conduct and to evaluate. The properties of UHPFRC specimens subjected to direct tension at high strain rates were studied in [14]. According to the results, the dissipated energy increases strongly in UHPFRC with increasing strain rate, and this predetermines it to be a promising cement-based material for impact- and blast-resistant applications.

The resistance of UHPFRC concrete slabs under contact explosions was tested in [15]. UHPFRC was chosen by the authors as a suitable material with less brittle behavior than normal-strength concrete. Slabs 120 mm in depth were subjected to contact explosions of 0.1 kg and 1.0 kg of TNT. Spallation and cratering of the specimens was observed, and was investigated quantitatively. UHPFRC slabs displayed significantly greater blast resistance capacity than NSC slabs.

The use of concrete as a soft layer in a multi-layer soft-hard-soft sandwich composite was studied in [16]. The more common and opposite hard-soft-hard composite was studied and used in a real application, see [17,18].


**Fig. 1.** Layout of the experiment.

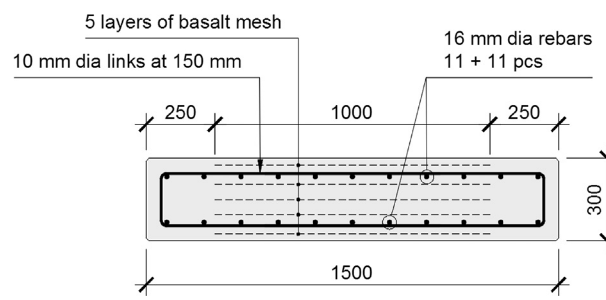


**Fig. 2.** Layout of Specimen No. 18.

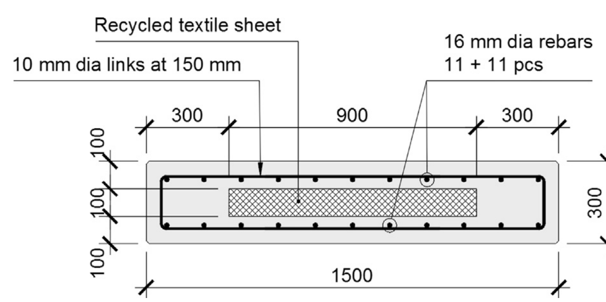


**Fig. 3.** Layout of Specimen No. 19.

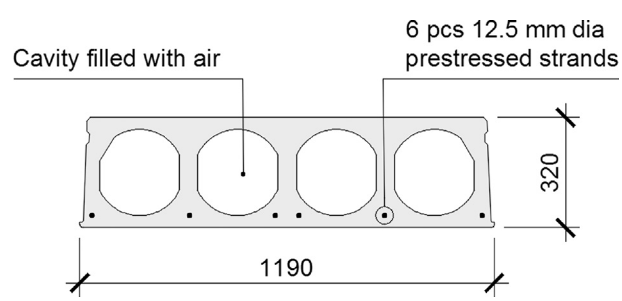


**Fig. 4.** Layout of Specimen No. 20.

Apart from the use of dispersed fiber reinforcement, another common approach aimed at improving the blast resistance of concrete is the introduction of additional reinforcement specifically designed to resist the high strain-rate dynamic loading associated with a blast event. Fine steel wire mesh (SWM) reinforcements were introduced [19–22]. Both static tests and field blast tests confirmed that the structure reinforced with a steel wire mesh had greatly improved material strength and ductility, together with reduced spalling.

Extensive research has been carried out in the field of resistance to

**Fig. 5.** Damage to reference specimen No. 1 after the blast. Top view (left), bottom view (right).

**Table 1**
Concrete properties of the specimens.

| Specimen No. | 18 | 19 | 20 |
|---|---|---|---|
| Compressive strength (cube) [MPa] | 77.9 | 78.3 | 63* |
| Flexural tensile strength [MPa] | 8.2 | 10.7 | 3.8* |
| 35 mm fibers [kg/m$^3$] | – | 80 | – |
| 13 mm fibers [kg/m$^3$] | 120 | 80 | – |

* Note: Minimal strength according to the manufacturer's certification.

multiple extreme loads acting either simultaneously or in a sequence, when the structure being loaded is already somehow influenced by a prior extreme load. The structure can be subject to a blast that causes a subsequent fire, or can be subject to a blast caused by fire. In these cases, the behavior of the structure will be influenced by the effects of prior exposure to high temperatures. For related research, see [23–26].

## 2. Experimental program

Full-scale testing is the most accurate method for determining the blast resistance of a complex heterogeneous material such as concrete or other cementitious composites. The current state-of-the-art in numerical modelling can provide reliable data on blast loading, but accurate calibration of material models always poses a challenge. The modelling always has to be supplemented with an experiment to verify the results obtained from the calculation.

The authors used their past experience in field testing of full-scale concrete specimens, and decided to use the same approach for hybrid concrete specimens made of concrete-based composite materials.

### *2.1. Layout of the experiment*

The experiments were performed in the Boletice military training area in fall 2015, in cooperation with the Armed Forces of the Czech Republic. The location and the layout of the experiment were very similar to those used in the authors' previous experiments [1–3], though some improvements were gradually made to the layout. A total of three specimens were tested; they were named no. 18 to no. 20, with respect to the history of the experimental program. Specimens no. 18 and 19 were concrete slabs 6 m in length, 1.5 m in width and 0.3 m in thickness, each with the same amount of steel reinforcement, i.e. 11 pcs ∅ 16 mm reinforcing bars every 140 mm on both surfaces, ∅ 10 mm every 150 mm as an outer transverse reinforcement. Concrete cover of 50 mm was taken to the surface of the transverse reinforcement. The arrangement of the reinforcement was essentially the same throughout the experiments.

Specimen no. 20 was a commercial hollow-core precast prestressed panel 6 m in length, 1.2 m in width and 0.32 m in thickness, defined by the manufacturer's program. Although the dimensions were not exactly the same, it can be assumed that the difference in width did not influence the behavior of the specimen during the experiment. The panel was reinforced only with 6 prestressing strands placed in the ribs. The panel contained no other reinforcement. Specimen no. 20 was included in the experiment as an example of a type of structural system widely used in building construction, in contrast with the other specimens, which represented structures specially designed for increased resistance to extreme loads. For the layouts of all the specimens, see Figs. 2–4.

The scheme of the experiment is shown in Fig. 1. The ground beneath the slabs was excavated to a depth of 2 m to avoid the results being influenced by the shock wave bouncing off the ground. 25 kg TNT charges were placed on steel chairs in the middle of each slab. The chairs provided 450 mm standoff from the slab.

A high-speed camera observed the spall formation on the soffit of the specimen through an angled mirror. In previous years, timber paneling had been introduced to postpone covering of the camera view by the enlarging fireball. However, a study of the recordings showed that the essential processes (mainly spall formation) occur before the fireball covers the camera view. The paneling is therefore not necessary, and it was not used in the experiments presented in this paper. The instrumentation of the experiment is more thoroughly described in [27,28]. This paper presents only the macroscopic findings of the experiments, the instrumental results will be subject to further publications.

### *2.2. Materials of the specimens*

The main motivation for the experimental program was to determine the effect of material heterogeneity. The composition of each

**Table 2**
Properties of the other materials present in the specimens.

| Material | Specimen No. | Characteristic properties |
|---|---|---|
| Steel (reinforcement) | 18, 19 | E = 200 GPa; $\sigma_y$ = 0.500 GPa; $\nu$ = *0.3;* ρ = 7850 kg/m$^3$ |
| Steel (prestressing) | 20 | E = 195 GPa; $\sigma_y$ = 1.860 GPa; $\nu$ = *0.3;* ρ = 7850 kg/m$^3$ |

E … Young's Modulus.
$\nu$ … Poisson's ratio.
$\sigma_y$ … yield strength.
ρ … weight density.

**Fig. 6.** Damage to specimen No. 18 after the blast. Overall view (top), top view (left), bottom view (right).


**Fig. 7.** Damage to specimen No. 19 after the blast. Overall view (top), top view (left), bottom view (right).

specimen was therefore unique, allowing a study to be made of multiple types of heterogeneity.

All specimens were made of concrete. Specimens No. 18 and No. 19 were made of fiber-reinforced concrete (FRC), and specimen no. 20 was made of standard concrete. Two types of high-strength steel (HSS) fibers were used: 35 mm in length, and 13 mm in length. The yield strength of the fiber material is guaranteed by the manufacturer to be higher than 2200 MPa. The compressive and tensile strength of the concrete, the fiber type and the fiber dosage for each specimen are summarized in Table 1. The material properties of the steel bar reinforcement and the prestressing cables are shown in Table 2.

Specimen no. 18 contained basalt fiber meshes in multiple layers along the depth of the specimen at distances of about 50 mm (Fig. 2). The melting point of the basalt fibers was 1350 °C. The tensile strength of the basalt fabric was about 4200 MPa, with a tensile modulus of elasticity of about 85 GPa. The unit weight of the mesh was 250 $g/m^2$, with weight density of 2.67 $g/cm^3$. Each string of the mesh consisted of multiple fibers, so the diameter of each string could not be accurately defined. From the parameters presented above, an effective area of each string equal to 1.4 $mm^2$ was calculated instead.

Specimen no. 19 contained two layers (50 mm) of recycled textile sheets with total thickness of 100 mm (Fig. 3). The textile sheets are


**Fig. 8.** Specimen No. 20, before (top) and after the blast (bottom).

**Table 3**
A comparison between the blast performance of the tested concrete slabs and reference specimen No. 1 [1].

| Specimen No. | 1* | 18 | 19 | 20 |
|---|---|---|---|---|
| Puncture – top surface | 0.43 m$^2$<br>100% | 0.26 m$^2$<br>60% | 0.25 m$^2$<br>58% | – |
| Concrete spalling (soffit) under thickness of concrete cover | 2.35 m$^2$<br>100% | 0.32 m$^2$<br>14% | 0.32 m$^2$<br>14% | – |
| Concrete spalling (soffit) greater than the thickness of concrete cover | 1.71 m$^2$<br>100% | 0.58 m$^2$<br>34% | 0.73 m$^2$<br>43% | – |
| Concrete spalling (top surface) under thickness of concrete cover | 0.43 m$^2$<br>100% | 0.15 m$^2$<br>35% | 0.16 m$^2$<br>37% | – |
| Concrete spalling (top surface) greater than the thickness of concrete cover | 0.43 m$^2$<br>100% | 0.26 m$^2$<br>60% | 0.25 m$^2$<br>58% | – |
| Concrete spalling (left side) under thickness of concrete cover | 0.52 m$^2$ | 0.00 m$^2$ | 0.00 m$^2$ | – |
| Concrete spalling (left side) greater than the thickness of concrete cover | 0.35 m$^2$ | 0.00 m$^2$ | 0.00 m$^2$ | – |
| Concrete spalling (right side) under thickness of concrete cover | 0.34 m$^2$ | 0.00 m$^2$ | 0.00 m$^2$ | – |
| Concrete spalling (right side) greater than the thickness of concrete cover | 0.23 m$^2$ | 0.00 m$^2$ | 0.00 m$^2$ | – |
| Volume of crushed concrete | 0.23 m$^3$<br>100% | 0.13 m$^3$<br>57% | 0.15 m$^3$<br>65% | – |
| Permanent deflection | 0.31 m<br>100% | 0.30 m<br>97% | 0.25 m<br>81% | – |

placed during casting of the specimen at 100 mm thick fresh concrete layer. Validation production experiments confirmed limited compressibility of the layers when loaded by the top 100 mm of fresh concrete layer. Specimen no. 20 had a hollow core filled only with air. Specimens no. 18 and no. 19 were reinforced with standard steel bars with a characteristic yield stress of 500 MPa.

Specimen no. 20 (Fig. 4) was reinforced only with 6 prestressing strands with a characteristic yield stress of 1860 MPa and a nominal diameter of 12.5 mm. No other reinforcement was present in the specimen.

### 2.3. Results of the experiment

The effects of blast loading on the top and bottom surfaces of the specimens are shown in Figs. 6–8, and in Table 3. The results for specimen No. 20 are not presented in the table due to total destruction of the specimen during the experiment (Fig. 8). To provide a comparison with experiments previously conducted by the authors, specimen No. 1, without any fibers, is used as a reference. It was tested in the first batch of experiments, published in Foglar and Kovar [1]. The reference specimen is made of standard reinforced concrete with compressive strength of 60.1 MPa and reinforced with the same steel bars as all the other specimens. The blast damage to the reference specimen is shown in Fig. 5.

Specimen No. 18 (Fig. 6; compressive strength of concrete 77.3 MPa; 120 kg/m$^3$ of fibers 13 mm in length; 5 layers of basalt mesh 30 x 30 mm distributed over the depth of the specimen) received considerably less damage than reference specimen No. 1. The punctured area was significantly reduced, as was the total volume of crushed concrete, which was only 0.13 m$^3$ (4.8% of the total volume of concrete). The punctured hole and crater in specimen No. 18 had roughly one half the extent of the damage to specimen No. 1. Apart from the flexural crack in mid-span, there was no apparent damage to the sides of the specimen. The residual permanent deflection of the specimen was approximately the same as the deflection of the reference specimen.

The significant increase in the blast resistance of specimen No. 18 can be ascribed to the increase in tensile strength of the concrete in comparison with the reference specimen. The effect of 5 layers of additional reinforcement in the form of a basalt mesh is apparent in the increased slope of the conical hole in the middle of the specimen. Specimen No. 15 (tested in 2014, Ref. [3]), with comparable material parameters, showed the angle of the ejected cone to be less than 45 degrees. Specimen No. 18 showed the angle to be more than 60 degrees. It seems that the addition of multiple layers of basalt fabric contributed to a significant reduction in the volume of concrete ejected after the blast.

Specimen No. 19 (Fig. 7; compressive strength of the concrete 66.9 MPa; 80 kg/m$^3$ of fibers 35 mm in length and 80 kg/m$^3$ of fibers 13 mm in length; a layer of recycled textile sheet in the middle of the specimen) showed very similar behavior to the previous specimen. The specimen showed slightly more spalling at the soffit, due to the absence of a basalt mesh in the concrete cover layer.

The overall size of the ejected fragments was found to be significantly greater than those of specimen No. 18. This seems to have been caused by the presence of the soft textile layer in the core of the specimen. Detailed analysis of the damage caused by the blast revealed a different mode of specimen failure than for all previously tested specimens. The primary damage to the soffit of all previous specimens with a more homogeneous structure was caused by the increased stresses on the lower surface caused by the rebound of the shock wave passing through the specimen. As a result of this loading, the concrete fragments were small, and they disconnected from the specimen with high velocity. The heterogeneity of the structure of specimen No. 19 with a soft textile core prevented the initial shock wave from reaching the soffit of the specimen, or at least delayed its arrival. High-speed camera recordings showed the response of the specimen soffit to blast load to be noticeably delayed in comparison with homogeneous specimens. The delay suggests that some processes occurred between the heterogeneous layers of materials. A further macroscopic study of the specimen revealed that the textile sheet layer was partially burnt off after the blast, and was partially compressed further inside the specimen. The compression of the soft middle layer created additional room for expanding explosion products, and the plastic deformation contributed to the dissipation of the blast energy. It was also observed that the thickness of the specimen was changed by the blast; the thickness was measured from the sides and at the breach. Some of the blast energy was also dissipated by the deformation of the top and bottom concrete layers.

Although it could not be accurately quantified from the results of the experiment, it can be assumed that the greater the weight of the fragments was, the lower was their velocity. The lethal range of the heavy fragments from specimen No. 19 would be shorter than the lethal range of the fragments from specimen No. 18.

Specimen No. 20 (Fig. 8; compressive strength of concrete 80 MPa; 6 no. prestressed strands dia. 12.5 mm, no other reinforcement; hollow core) was completely destroyed by the blast. An analysis of the debris showed that the most common mode of failure was the formation of cracks along the thinnest parts of the cross section around the voids. The shock wave passing through the specimen concentrated in the area between the voids and created areas of increased stresses. The concrete failed in these areas due to the lack of any reinforcement covering the tensile stresses.

The experiment confirmed the presumed extremely brittle behavior of a standard hollow core prestressed panel. Other tested specimens were also damaged, but even after the blast they offered considerable residual load-bearing capacity. The hollow core specimen was completely destroyed. It is obvious from the results that this kind of structure is not suitable for any application where it may be subjected to high-velocity loading.

Specimen no. 20 clearly does not follow the line of the previous experiments, and its behavior cannot be compared with the previous experiments, because of the significant difference in the composition of the specimen. An important consideration is that this specimen is an example of a typical structure used in construction, a typical structure that was not designed with blast resistance in mind, a typical structure that would most likely be targeted in a terrorist attack in a developed country.

Both composite specimens (nos. 18 and 19) exhibited higher resistance to blast than normal concrete reference specimen no. 1. The damaged area of the composite specimens was approximately one half of the damaged area of the reference specimen. The higher blast resistance can be ascribed partly to the increased compressive and tensile strength of the concrete, and partly to the heterogeneity of the composite specimens.

A detailed study of the damage to specimens nos. 18 and 19 caused by the close-in explosion found some apparent delamination of the concrete matrix in both specimens. This seems to have been caused by the internal rebound of the shock wave, which causes a local increase in the stresses inside the specimen. This finding will be verified by numerical modelling in the ongoing research.

## 3. Conclusions

This paper has presented the results of full-scale blast experiments designed to characterize the resistance of concrete-based composite bridge decks subjected to close-in blast loading. Three composite decks with different degrees of heterogeneity were proposed and tested. In previous experiments, the authors progressed from standard reinforced concrete to fiber-reinforced concrete, while trying to introduce more ductile behavior into the material. The use of composite materials was chosen as a logical step to further increase the blast resistance of concrete structures.

Additional materials were embedded inside the concrete matrix. A basalt mesh inserted into the concrete takes over the tensile stresses, acting similarly to standard reinforcing bars. The mesh improved the blast performance, as expressed by the area of spalling and by the volume of debris. The mesh was able to hold, or at least to slow down, the parts of the specimen ejected by the explosion, thanks to the small distance between its strings. Another way radically to increase the heterogeneity of the concrete was to introduce soft textile sheets into the core of the specimen.

A detailed macroscopic study of the damage to the specimen caused by the close-in explosion found apparent delamination of both tested composite specimens. The delamination seems to be the result of stress concentration caused by the internal rebound of the shock wave at the interface between materials with varying densities. This delamination can benefit the overall blast performance of the structure. In fact, the increased delamination and the increased deformation of the concrete cover can be very effective in dissipating the blast energy. The formation of a massive horizontal crack across a wide area requires a great deal of mechanical energy. In combination with the subsequent plastic deformation of the cover layer being restrained by the basalt mesh, a large amount of blast energy is mitigated within the structure of the proposed composite bridge deck.

## Acknowledgement

Financial support from the Czech Science Foundation (GACR) project no. 17-23067S is gratefully acknowledged.

## References

[1] Foglar M, Kovar M. Conclusions from experimental testing of blast resistance of FRC and RC bridge decks. Int J Impact Eng 2013;59:18–28. https://doi.org/10.1016/j.ijimpeng.2013.03.008.

[2] Foglar M, Hajek R, Kovar M, Štoller J. Blast performance of RC panels with waste steel fibers. Constr Build Mater 2015;94:536–46. https://doi.org/10.1016/j.conbuildmat.2015.07.082. art. no. 6897.

[3] Foglar M, Hajek R, Fladr J, Pachman J, Stoller J. Full-scale experimental testing of the blast resistance of HPFRC and UHPFRC bridge decks. Constr Build Mater 2017;145:588–601. https://doi.org/10.1016/j.conbuildmat.2017.04.054.

[4] Hajek R, Foglar M. Numerical and experimental analysis of the effect of rigid barriers on blast wave propagation. ASCE J Struct Eng 2015;141(12). https://doi.org/10.1061/(ASCE)ST.1943-541X.0001308.

[5] Hájek R, Foglar M, Fládr J. Influence of barrier material and barrier shape on blast wave mitigation. Constr Build Mater 2016;120:54–64. https://doi.org/10.1016/j.conbuildmat.2016.05.078. ISSN 0950-0618.

[6] Dear JP, Rolfe E, Kelly M, Arora H, Hooper PA. Blast performance of composite sandwich structures. Procedia Eng 2016;173:471–8. https://doi.org/10.1016/j.proeng.2016.12.065.

[7] Arora H, Del Linz P, Dear JP. Damage and deformation in composite sandwich panels exposed to multiple and single explosive blasts. Int J Impact Eng 2017;104:95–106. https://doi.org/10.1016/j.ijimpeng.2017.01.017.

[8] Kerber A, Gargano A, Pingkarawat K, Mouritz AP. Explosive blast damage resistance of three-dimensional textile composites. Compos A 2017;100:170–82. https://doi.org/10.1016/j.compositesa.2017.05.005.

[9] Tabatabaei ZS, Volz JS, Baird J, Gliha BP, Keener DI. Experimental and numerical analyses of long carbon fiber reinforced concrete panels exposed to blast loading. Int J Impact Eng 2013;57:70–80. ISSN 0734-743X.

[10] Magnusson J. Fiber reinforced concrete beams subjected to air blast loading. Int J Nordic Concr Res 2006;35:1–17.

[11] Lan S, Tat-Seng Lok TS, Heng L. Composite structural panels subjected to explosive loading. Constr Build Mater 2005;9(5):387–95. ISSN 0950-0618.

[12] Yusof MA, Norazman N, Ariffin A, Zain FM, Risby R, Ng CP. Normal strength steel fiber reinforced concrete subjected to explosive loading. Int J Sustain Constr Eng Technol 2010;1(2):127–36. ISSN 2180-3242.

[13] Luccioni B, Isla F, Codina R, Ambrosini D, Zerbino R, Giaccio G, et al. Effect of steel fibers on static and blast response of high strength concrete. Int J Impact Eng 2017;107:23–37. https://doi.org/10.1016/j.ijimpeng.2017.04.027.

[14] Pyo S, El-Tawil S, Naaman AE. Direct tensile behavior of ultra high performance fiber reinforced concrete (UHP-FRC) at high strain rates. Cem Concr Res 2016;88:144–56.

[15] Li J, Wu C, Hao H, Wang Z, Su Y. Experimental investigation of ultra-high performance concrete slabs under contact explosions. Int J Impact Eng 2016;93:62–75.

[16] Wu J, Liu X, Hoe Chew S. Parametric study on cement-based soft-hard-soft (SHS) multi-layer composite pavement against blast load. Constr Build Mater 2015;98:602–19. https://doi.org/10.1016/j.conbuildmat.2015.08.046.

[17] Richard Liew JY, Yan J-B, Huang Z-Y. Steel-concrete-steel sandwich composite structures – recent innovations. J Constr Steel Res 2017;130:202–21. https://doi.org/10.1016/j.jcsr.2016.12.007.

[18] Christian A, Ong Khim Chye G. Performance of fiber reinforced high-strength concrete with steel sandwich composite system as blast mitigation panel. Procedia Eng 2014;95:150–7. https://doi.org/10.1016/j.proeng.2014.12.174.

[19] Li J, Wu C, Hao H, Su Y, Li Z. A study of concrete slabs with steel wire mesh reinforcement under close-in explosive loads. Int J Impact Eng 2017. https://doi.org/10.1016/j.ijimpeng.2017.01.016. (in press).

[20] Li J, Wu C, Liu Z. Comparative evaluation of steel wire mesh, steel fibre and high performance polyethylene fibre reinforced concrete slabs in blast tests. Thin-Walled Struct 2017. https://doi.org/10.1016/j.tws.2017.05.023. (in press).

[21] Li J, Wu C, Hao H, Su Y. Experimental and numerical study on steel wire mesh reinforced concrete slab under contact explosion. Mater Des 2017;116:77–91. https://doi.org/10.1016/j.matdes.2016.11.098.

[22] Wu C, Li J. Structural protective design with innovative concrete material and retrofitting technology. Procedia Eng 2017;173:49–56. https://doi.org/10.1016/j.proeng.2016.12.020.

[23] Yoo D-Y, Banthia N. Mechanical and structural behaviors of ultra-high-performance fiber-reinforced concrete subjected to impact and blast. Constr Build Mater 2017;149:416–31.

[24] Li J, Wu C, Hao H, Liu Z. Post-blast capacity of ultra-high performance concrete columns. Eng Struct 2017;134:289–302. https://doi.org/10.1016/j.engstruct.2016.12.057.

[25] Guo Z, Chen W, Zhang Y, Zou H. Post fire blast-resistances of RPC-FST columns using improved Grigorian model. Int J Impact Eng 2017;107:80–95. https://doi.org/10.1016/j.ijimpeng.2017.05.005.

[26] Pantelides CP, Garfield TT, Richins WD, Larson TK, Blakeley JE. Reinforced concrete and fiber reinforced concrete panels subjected to blast detonations and post-blast static tests. Eng Struct 2014;76:24–33. https://doi.org/10.1016/j.engstruct.2014.06.040.

[27] Hajek R, Kovar M, Foglar M, Pachman J, Stoller J. Field testing of concrete members subjected to contact and adjacent blast. Adv Mater Res 2015;1106:164–7. https://doi.org/10.4028/www.scientific.net/AMR.1106.164.

[28] Foglar M, Pachman J, Pelikan V, Kunzel M, Kovar M. The structural response of a reinforced concrete specimen subjected to adjacent blast loading. WIT Trans Built Environ 2014;141:171–9. ISBN 978-1-84564-796-4.